

The effect of particle size and nitric acid uptake on the homogeneous freezing of aqueous sulfuric acid particles

Azadeh Tabazadeh

NASA Ames Research Center, Moffett Field, CA

Scot T. Martin

Department of Environmental Sciences and Engineering, University of North Carolina, Chapel Hill, NC

Jin-Sheng Lin

Bay Area Environmental Research Institute, San Francisco, CA

Abstract. Recent laboratory data on ice freezing from aqueous H₂SO₄ solutions are used to update our homogeneous ice freezing nucleation algorithm. The effect of particle size on the ice freezing process is demonstrated by calculating and comparing ice freezing curves for different size particles ranging from 0.2 to 4 micron in radius. Using the ice nucleation model we show that liquid water saturation is required above -44°C to activate submicron H₂SO₄ particles into cloud droplets. A thermodynamic model is used to show that the available laboratory data on ice freezing from ternary H₂SO₄/HNO₃/H₂O solutions are insufficient to adequately address the effect of HNO₃ uptake on the homogeneous freezing of aqueous H₂SO₄ particles into ice.

Introduction

Ice clouds play important roles in Earth's climate [Ramanathan *et al.*, 1983] and chemistry Solomon [1990]. One mechanism that has been suggested to initiate ice cloud nucleation in the atmosphere is homogeneous freezing of aqueous H₂SO₄ solution droplets [Sassen and Dodd, 1989; DeMott *et al.*, 1994; Jensen *et al.*, 1994; Heymsfield and Miloshevich, 1995; Demott *et al.*, 1997]. However, the ice freezing process through this mechanism is complicated by the fact that a significant fraction of gas phase HNO₃ will partition into sulfate aerosols near the ice freezing point of the solution [Tabazadeh *et al.*, 1994; Carslaw *et al.*, 1994].

The ice freezing curve in aqueous H₂SO₄ droplets was recently measured by Koop *et al.* [1998]. The ice freezing temperatures determined by Bertram *et al.* [1996] for aqueous H₂SO₄ droplets, which we previously used to parameterize our ice nucleation model [Tabazadeh *et al.*, 1997 a, b], appear to be systematically too high [Koop *et al.*, 1998]. In addition, differential scanning calorimetry has recently been used to determine the ice freezing curve in aqueous HNO₃ and ternary H₂SO₄/HNO₃/H₂O droplets [Chang *et al.*, 1999]. In this work we use recent laboratory measurements on ice freezing from binary and ternary solution droplets [Koop *et al.*, 1998; Chang *et al.*, 1999], along with new surface tension data on the aqueous H₂SO₄ system [Myhre *et al.*, 1998], to update our homogeneous ice freezing nucleation algorithm.

Model Update

Figure 1 shows critical ice saturations expected to nucleate ice in aqueous H₂SO₄, HNO₃ and ternary H₂SO₄/HNO₃/H₂O solutions as a function of the ambient water vapor pressure based on recent laboratory measurements. The data of Koop *et al.* [1998] and Bertram *et al.* [1996] show very different behaviors for the freezing of ice from aqueous H₂SO₄ solution droplets. The main objective of this paper is to update our ice nucleation model to agree with more recent measurements.

An interesting feature of Figure 1 is that the ice freezing curves for both aqueous H₂SO₄ and HNO₃ solution droplets are nearly identical. According to equilibrium model calculations [Tabazadeh *et al.*, 1994; Carslaw *et al.*, 1994], the ionic strengths of H₂SO₄/H₂O and HNO₃/H₂O at the same relative

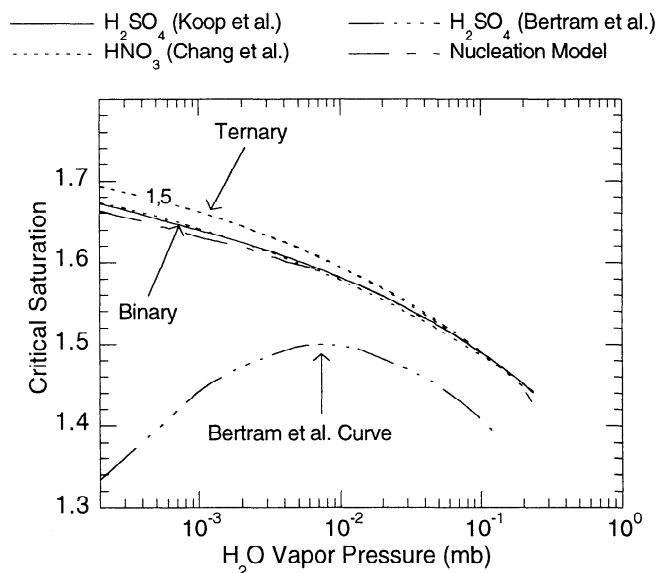


Figure 1. The variation of critical ice saturation as a function of water partial pressure over the solution. The solid and dotted curves are calculated directly from the tabulated relations given in Koop *et al.* [1998] and Chang *et al.* [1999]. The numbers on the dotted lines give the H₂SO₄ content of a ternary HNO₃/H₂SO₄/H₂O aerosol in weight percent. The solid dotted curve is based on the data of Bertram *et al.* [1996] converted to an appropriate form using the method described in Tabazadeh *et al.* [1997a]. Also shown are the results of our ice nucleation model for a 4 micron aqueous H₂SO₄ particle.

humidity are similar in magnitude. Since the equilibrium freezing point depression is often directly proportional to the ionic strength, the fact that the two binary electrolytes have similar ice freezing kinetics is at least partially rationalized.

Also shown in Figure 1 are the ice freezing curves for $\text{H}_2\text{SO}_4/\text{HNO}_3/\text{H}_2\text{O}$ ternary solutions, which contain 1 and 5% H_2SO_4 by weight [Chang *et al.*, 1999]. The slight (< 2%) increase in the critical ice saturation in a ternary solution, as compared to the binary systems, is rationalized by the increase in entropy of the solution as a result of mixing. Below we use a thermodynamic model to show that the current laboratory data on ice freezing from ternary solutions are insufficient to adequately address the effect of HNO_3 uptake (by sulfate aerosols) on the ice formation process in the atmosphere.

Denoting V_d (cm^3) and w_s as the volume and weight percent of a H_2SO_4 solution droplet, the rate of ice nucleation (particle sec^{-1}) at a given temperature is:

$$J = C(T, w_s, V_d) \text{EXP} \left[\frac{-\Delta F_g(T, w_s) - \Delta F_{act}(T, w_s)}{kT} \right] \quad (1)$$

where C (particle sec^{-1}) is the preexponential factor, ΔF_g (ergs) is the Gibbs free energy for the formation of the ice germ, ΔF_{act} (ergs) is the diffusion activation energy of water molecules across the ice/sulfate solution phase boundary, and k is the Boltzmann constant. The preexponential factor and the Gibbs free energy are estimated as follows:

$$C(T, w_s, V_d) \cong 2.1 \times 10^{33} V_d \sqrt{\sigma_{sul/ice}(w_s, T) T} \quad (2)$$

$$\Delta F_g = \frac{4}{3} \pi \sigma_{sul/ice} r_g^2 \quad (3)$$

where $\sigma_{sul/ice}$ is the interface energy between the ice/sulfate solution and r_g (cm) is the critical germ radius. For our purposes, an ice freezing event occurs when $J = 1$ particle sec^{-1} .

We previously described [Tabazadeh *et al.*, 1997 a, b] how the equations (1) through (3) can be used to extract a numerical relation for the variation of activation free energy of water

molecules in solution based on laboratory ice freezing data. We follow the same procedure here to derive a new relation for the activation free energy of water molecules in solution based on the ice freezing data of Koop *et al.* [1998].

In deriving an expression for the activation free energy, we generated two fittings of the activation energy function for particle sizes of 1.55 and 6.3 micron in radius that bracket the laboratory size range [Koop *et al.*, 1998]. The final activation energy relation reported in Table 1 is obtained by averaging the two expressions above for different particle size assumptions. In addition, we replaced the surface tension relation in the model by a new expression based on recent laboratory measurements by Myhre *et al.* [1998]. All the functions required for the nucleation calculations are described and summarized in Table 1. The nucleation model calculates a unique solution for the ice freezing temperature of a given size droplet as a function of only the ambient water vapor pressure.

Atmospheric Implications

Figure 2 shows the effect of particle size on ice nucleation from an aqueous H_2SO_4 solution droplet. The size-dependence calculated by our model is in good agreement with the size-dependence measured in the laboratory for ice nucleation in pure supercooled water droplets (see Figure 2 in Pruppacher [1995]). As expected, due to smaller volumes (V_d term in equation 1), higher ice saturations are needed to form ice in submicron atmospheric particles as compared to micron-sized aerosols studied in the laboratory [Koop *et al.*, 1998]. Recent measurements [Chen *et al.*, 2000] support our calculations that submicron sulfate particles freeze at lower temperatures as compared to micron-sized particles.

Laboratory freezing data on submicron water droplets indicate that such droplets can often remain supercooled to temperatures near and sometimes below -40°C [Hagen *et al.*, 1981; Pruppacher, 1995]. Thus the fact that our ice nucleation model calculates a liquid water activation temperature below -40°C for submicron aqueous H_2SO_4 particles (Figure 2) is not surprising since the effect of solute is to further depress the freezing point of ice in solution beyond that of a pure supercooled water droplet. Overall, a nucleation model offers

Table 1. Ice Nucleation Functions

Latent heat of melting in erg mol^{-1} (T is in K): $L_m(T) = 10^7 [6005.2356 + 18.2719(T - 273.15) - 0.06354(T - 273.15)^2]$

Ice density (T is in K): $\rho_{ice}(T) = 0.916 - 8.75 \times 10^{-5}(T - 273.15) - 1.667 \times 10^{-7}(T - 273.15)^2$

Sulfate solution/air interface energy based on the data of Myhre *et al.* [1998] in dyn cm^{-1} (where w is the H_2SO_4 weight percent of the solution):

$\sigma_{sul/air}^{180} = 85.75507114 + 9.541966318 \times 10^{-2} w - 1.103647657 \times 10^{-1} w^2 + 7.485866933 \times 10^{-3} w^3 - 1.912224154 \times 10^{-4} w^4 + 1.736789787 \times 10^{-6} w^5$

$\sigma_{sul/air}^{220} = 82.01197792 + 5.312072092 \times 10^{-1} w - 1.050692123 \times 10^{-1} w^2 + 5.415260617 \times 10^{-3} w^3 - 1.145573827 \times 10^{-4} w^4 + 8.969257061 \times 10^{-7} w^5$

$\sigma_{sul/air}^{260} = 77.40682664 - 6.963123274 \times 10^{-3} w - 9.682499074 \times 10^{-3} w^2 + 8.87979880 \times 10^{-4} w^3 - 2.384669516 \times 10^{-5} w^4 + 2.095358048 \times 10^{-7} w^5$

For $180 \leq T \leq 220$ K, $\sigma_{sul/air}^T = \sigma_{sul/air}^{220} + (5.5 - 0.025T)(\sigma_{sul/air}^{180} - \sigma_{sul/air}^{220})$

For $220 < T \leq 260$ K, $\sigma_{sul/air}^T = \sigma_{sul/air}^{260} + (6.5 - 0.025T)(\sigma_{sul/air}^{220} - \sigma_{sul/air}^{260})$

Diffusion activation energy $\times 10^{13}$ in ergs derived from the Koop *et al.* [1998] ice nucleation data (T is in K):

For $T < 220$ K, $\Delta F_{act} = -17459.516183 + 458.45827551T - 4.8492831317T^2 + 0.026003658878T^3 - 7.1991577798 \times 10^{-5}T^4$

$+ 8.9049094618 \times 10^{-8}T^5 - 2.4932257419 \times 10^{-11}T^6$

For $T > 220$ K, $\Delta F_{act} = 104525.93058 - 1103.7644651T + 1.070332702T^2 + 0.017386254322T^3 - 1.5506854268 \times 10^{-6}T^4$

$- 3.2661912497 \times 10^{-8}T^5 + 6.467954459 \times 10^{-10}T^6$

Equilibrium sulfuric acid weight percent composition and water saturation vapor pressure: See Tabazadeh *et al.* [1997a]

Sulfuric acid solution density: See Myhre *et al.* [1998]

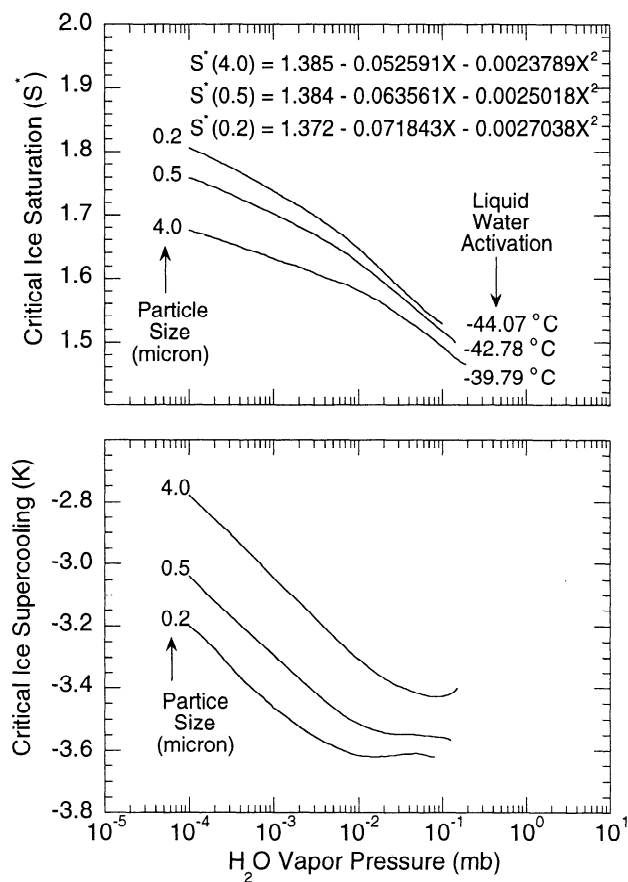


Figure 2. The variation of the critical ice saturation (and supercooling) as a function of water partial pressure and particle size in radius calculated using the ice nucleation model. The critical supercooling is defined as the difference between the critical ice freezing temperature and the ice frost point of the solution. Liquid water activation temperatures marked on the plot show transition temperatures above which particles activate into liquid water droplets prior to freezing into ice. The variable X in the above equation is $\ln(PH_2O)$, where PH_2O is the ambient water vapor pressure in mb.

several advantages compared to parameterizations for treating the ice formation process in the atmosphere. Simple parameterizations tend to provide information that is exclusive to one size particle, whereas in the atmosphere ice nucleation in principle occurs over an entire submicron aerosol particle size distribution.

Liquid water activation temperatures marked in Figure 2 (for three different particle sizes) show transition temperatures above which sulfate particles will first activate into liquid water droplets prior to freezing into ice. To accurately predict this transition point in the atmosphere is important since cirrus ice clouds that first go through a liquid water activation phase are often composed of a large population of small ice crystals [Jensen et al., 1998]. Radiative properties of cirrus clouds are strongly affected by the number of ice particles nucleated [Jensen and Toon, 1994]. The results of our calculations show that submicron H_2SO_4 particles in the atmosphere can remain supercooled to temperatures near -44 °C. Therefore it is likely that above -44 °C cirrus ice clouds often form by first going through a liquid water activation phase provided that they are devoid of heterogeneous solid impurities [Martin, 1998; Demott et al., 1997].

The composition of an aqueous H_2SO_4 solution droplet in the atmosphere is altered by the uptake of HNO_3 . In Figure 3 the change in the ternary solution composition as a function of temperature is shown for three selected water vapor pressure profiles, which bracket typical conditions in the lower stratosphere and upper troposphere. The shaded area shows the range of H_2SO_4 compositions of ternary systems for which the ice freezing properties of solutions have been determined in the laboratory [Chang et al., 1999].

Ternary solution droplets containing between 1 to 5 wt % H_2SO_4 freeze at ice saturations near that of the binary systems [Chang et al., 1999, see Figure 1]. In the background stratosphere the H_2SO_4 weight percent in solution near the ice nucleation point is located within the gray area for which the ice freezing properties of ternary solutions have been studied in the laboratory. Thus the effect of HNO_3 uptake in depressing the ice freezing temperature is negligible (Figure 1) if the stratosphere is in a background state (Figure 3). However, for a volcanically perturbed state, where H_2SO_4 mixing ratios are higher, the H_2SO_4 weight percent of a ternary solution near the ice freezing point is close to 15 % (Figure 3). Because this

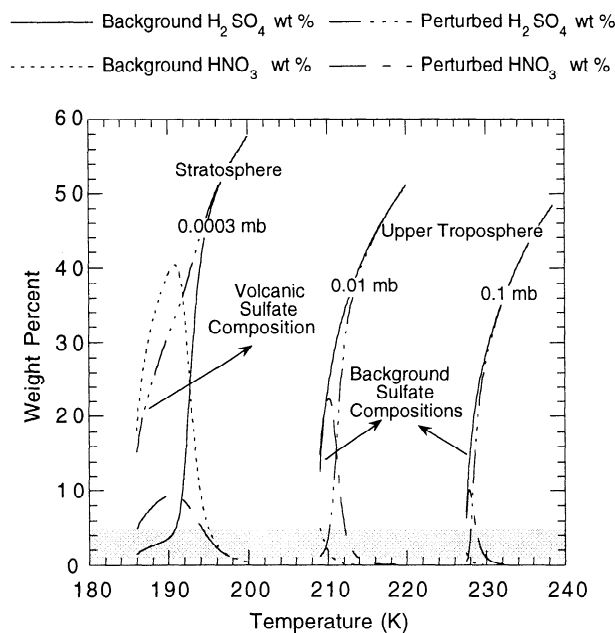


Figure 3. The variation of ternary $H_2SO_4/HNO_3/H_2O$ aerosol composition with temperature for different water vapor pressure regimes based on the thermodynamic relations given in Luo et al. [1995]. The 0.1 and 0.01 mb curves are calculated for a constant H_2SO_4 atmospheric mixing ratio of 100 ppt and variable HNO_3 atmospheric mixing ratios of 0.1 (background) and 2 ppb (perturbed by convective pollution) at 200 mb. The 0.0003 mb curves are calculated for a constant HNO_3 atmospheric mixing ratio of 10 ppb and variable H_2SO_4 mixing ratios of 0.5 (background) and 20 ppb (perturbed by volcanic eruptions) at 60 mb. The calculations were performed down to about -3.2 K below the equilibrium ice condensation point of the solution. The shaded area shows the range of H_2SO_4 compositions in ternary aerosol solutions for which the ice freezing properties of ternary systems have been measured in the laboratory [Chang et al., 1999]. The arrows in the plot refer to H_2SO_4 composition in ternary solutions for which laboratory ice freezing data are lacking. Laboratory freezing data for ternary solutions are currently unavailable for volcanic and background conditions in the stratosphere and upper troposphere, respectively.

ternary composition regime has not been studied in the laboratory, it is difficult to compare and contrast the effect of HNO₃ uptake on the ice freezing process in the stratosphere between the two cases. Satellite data indicate that it may be more difficult to freeze aerosols in a volcanically perturbed environment as compared to a background state [Santee *et al.*, 1998]. Thus additional laboratory data are needed to better understand how volcanic eruptions may affect the ice formation process in the lower stratosphere.

Similarly in the upper troposphere the laboratory data on ice freezing from ternary systems are insufficient to adequately describe and compare the differences between the background and perturbed states. For example, in a polluted upper troposphere HNO₃ mixing ratios reach values as high as 2 ppbv [Laaksonen *et al.*, 1997; Schnieder *et al.*, 1998]. The high levels of HNO₃ in the upper troposphere are linked to dry convection that injects polluted boundary layer air directly into the upper troposphere. The H₂SO₄ weight percent of ternary solutions in a polluted upper troposphere are located within the gray shaded area (see Figure 3). On the other hand, ice freezing curves for a background state (between 8 to 12% H₂SO₄ and 1 to 5 % HNO₃ by weight), containing about 100 pptv of HNO₃, have not yet been explored in the laboratory (Figure 3). Thus it is difficult to address the question of how convection (leading to high levels of HNO₃) may affect cirrus formation in the upper troposphere when no information is available on ice freezing properties for compositions representative of the background state (~100 pptv of HNO₃).

Summary

We updated our homogeneous ice freezing nucleation code using recent laboratory measurements. Our results indicate that ice freezing curves for submicron aerosol particles are significantly different than those determined in the laboratory for micron-sized particles. Further we show that in the atmosphere, for temperatures above -44 °C, submicron aqueous H₂SO₄ particles will activate into liquid water droplets prior to freezing into ice. Finally the available laboratory data on ice freezing from H₂SO₄/HNO₃/H₂O solutions are insufficient to address how HNO₃ uptake by aqueous H₂SO₄ particles may affect the ice formation process in the atmosphere.

Acknowledgments. We thank N. Larsen and A. Ravishankara for helpful comments on the paper. We also thank Paul Demott and Luisa Molina for sending us preprints of their work on ice nucleation. This work was mainly supported by NASA's Atmospheric Chemistry Modeling and Analysis Program. AT and STM acknowledge support from Presidential Early Career Awards for Scientists and Engineers. STM is grateful for support received from the NSF Atmospheric Chemistry Program, the Petroleum Research Fund, and the Defense University Research Instrumentation Program. Send email to AT for a computer copy of the ice nucleation model.

References

Bertram, A. K., D. D. Patterson, and J. J. Sloan, Mechanisms and temperature for the freezing of sulfuric acid aerosols measured by FTIR extinction spectroscopy, *J. Phys. Chem.*, **100**, 2376, 1996.
 Carslaw, K. S., B. P. Luo, S. L. Clegg, T. Peter, P. Brimblecombe, and P. Crutzen, Stratospheric aerosol growth and HNO₃ gas phase depletion form coupled HNO₃ and water uptake by liquid particles, *Geophys. Res. Lett.*, **21**, 2479, 1994.
 Chang, H. A., T. Koop, L. T. Molina, and M. J. Molina, Phase transition

in emulsified HNO₃/H₂O and HNO₃/H₂SO₄/H₂O solutions, *J. Phys. Chem.*, **103**, 2673-2679, 1999.
 Chen, Y., et al., Ice formation by sulfate and sulfuric acid particles under upper tropospheric condition, *J. Atmos. Sci.*, in press.
 DeMott, P. J., M. P. Meyers, and W. R. Cotton, Parameterization and impact of ice initiation processes relevant to numerical model simulations of cirrus clouds, *J. Atmos. Sci.*, **51**, 77, 1994.
 DeMott, P. J., D. C. Rogers, and S. M. Kreidenweis, The susceptibility of ice formation in the upper troposphere to insoluble aerosol components, *J. Geophys. Res.*, **102**, 19575, 1997.
 Hagen, D. E., R. J. Anderson, J. L. Kassner, Homogeneous condensation-freezing nucleation rate measurements for small water droplets in an expansion cloud chamber, *J. Atmos. Sci.*, **38**, 1236, 1981.
 Heymsfield, A. J., and L. M. Miloshevich, Relative humidity and temperature influences on cirrus formation and evolution: Observations from wave clouds and FIRE II, *J. Atmos. Sci.*, **52**, 4302, 1995.
 Jensen, E. J., O. B. Toon, D. L. Westphal, S. Kinne, and A. J. Heymsfield, Microphysical modeling of cirrus I. Comparison with 1986 FIRE IFO measurements, *J. Geophys. Res.*, **99**, 10,421, 1994.
 Jensen, E. J., and O. B. Toon, Ice nucleation in the upper troposphere: Sensitivity to aerosol number density, temperature, and cooling rate, *Geophys. Res. Lett.*, **18**, 2019, 1994.
 Jensen, E., et al., Ice nucleation processes in upper tropospheric wave-clouds observed during SUCCESS, *Geophys. Res. Lett.* **25**, 1367, 1998.
 Koop, T. H. P. Ng., L. T. Molina, and M. J. Molina, A new optical technique to study aerosol phase transition: The nucleation of ice from H₂SO₄ aerosols, *J. Phys. Chem.*, **102**, 8924, 1998.
 Laaksonen, A., J. Hienola, M. Kulmala, and F. Arnold, Supercooled cirrus clouds formation modified by nitric acid pollution of the upper troposphere, *Geophys. Res. Lett.*, **24**, 3009, 1997.
 Luo, B., et al., Vapor pressures of H₂SO₄/HNO₃/HCl/HBr/H₂O solutions to low stratospheric temperatures, *Geophys. Res. Lett.*, **22**, 247, 1995.
 Martin, S. T., Phase Transformation of the ternary system (NH₄)₂SO₄-H₂SO₄-H₂O and the implications for cirrus cloud formation, *Geophys. Res. Lett.*, **25**, 1657, 1998.
 Myhre, C. E. L., C. J. Nielsen, and O. W. Sasstad, Density and surface tension of aqueous H₂SO₄ at low temperatures, *J. Chem. Eng. Data*, **43**, 617, 1998.
 Pruppacher, H. R., A new look at homogenous ice nucleation in supercooled water drops, *J. Atmos. Sci.*, **52**, 1924, 1995.
 Ramanathan, V., E. J. Pitcher, R. C. Malone and L. Blackman, The response of a spectral general circulation model to refinements in radiative processes, *J. Atmos. Sci.*, **40**, 605, 1983.
 Santee, M. L., A. Tabazadeh, G. L. Manney, R. J. Salawitch, L. Froidevaux, W. G. Read, and J. W. Waters, UARS MLS HNO₃ observations: Implications for Antarctic PSCs, *J. Geophys. Res.*, **103**, 13,285, 1998.
 Sassen, K., and G. C. Dodd, Haze particle nucleation simulations in cirrus clouds, and applications for numerical and lidar studies, *J. Atmos. Sci.*, **46**, 3005, 1989.
 Schnieder, J., et al., Nitric acid (HNO₃) in the upper troposphere and lower stratosphere at mid latitudes: New results from aircraft-based mass spectrometric measurements, *J. Geophys. Res.*, **103**, 25,337, 1998.
 Solomon, S., Progress towards a quantitative understanding of Antarctic ozone depletion, *Nature*, **347**, 1990.
 Tabazadeh, A., R. P. Turco, K. Drdla, M. Z. Jacobson, and O. B. Toon, A study of Type I polar stratospheric cloud formation, *Geophys. Res. Lett.*, **21**, 1619, 1994b.
 Tabazadeh, A., E. Jensen, and O. B. Toon, A model description for cirrus cloud nucleation from homogeneous freezing of sulfate aerosols, *J. Geophys. Res.*, **102**, 23,845, 1997a.
 Tabazadeh, A., O. B. Toon, and E. Jensen, Formation and implications of ice particle nucleation in the stratosphere, *Geophys. Res. Lett.*, **24**, 2007, 1997b.

J. Lin, NASA Ames Research Center, MS 245-4, Moffett Field, CA 94035-1000 (lin@sky.arc.nasa.gov).

S. Martin, University of North Carolina at Chapel Hill, Chapel Hill, NC 27599-7400 (scot_martin@unc.edu).

A. Tabazadeh, NASA Ames Research Center, MS 245-4, Moffett Field, CA 94035-1000 (atabazadeh@mail.arc.nasa.gov).

(Received August 2, 1999; Revised January 25, 2000; Accepted: February 24, 2000)